Journal of the Korean Ceramic Society
Vol. 45, No. 12, pp. 788~795, 2008.

Long-term Testing and Analysis of a ScSZ / LaSrCuFe Cell

Jürgen Wackerl†, Dong-Hyun Peck*, and Torsten Markus

Forschungszentrum Jülich GmbH, 52425 Jülich, Germany
**Korea Institute of Energy Research, 305-343 Daejeon, Korea*
(Received October 20, 2008; Revised December 30, 2008; Accepted December 30, 2008)

ABSTRACT

An electrolyte supported SOFC cell was tested at 800°C in air for 3600 h with an applied current density of 200 mA/cm² to examine possible cathode degradation issues. A scandium- stabilized zirconia (ScSZ) with additional manganese doping (ScSZ: Mn) was used as electrolyte. A strontium and copper-doped lanthanum ferrite (LaSrCuFe) and platinum were used as cathode and quasi-anode material, respectively. The DC resistance was logged over the complete testing period. Additionally, impedance spectroscopy was used from time to time to track changes of the cell in-situ. Post-test analysis of the cell using methods like scanning electron microscopy imaging and other electrochemical testing methods allow the identification of different degradation sources. The results indicate a promising combination of electrolyte and cathode material in terms of chemical compatibility and electrical performance.

***Key words*: Scandia doped zirconia, Perovskite, Degradation, Cell test, Impedance spectroscopy**

1. Introduction

In times of increasing fossil fuel costs, the demand of high efficient energy conversion technology is increasing. One of these technologies is the solid oxide fuel cell (SOFC), converting fuel and therefore chemical energy to electrical one without the intermediate step of mechanical energy like rotation, as it was required in combustion techniques like gas turbines. However, the classical materials used for SOFC require a high operating temperature to be economical interesting. One of the classical materials is the yttria-stabilized zirconia (YSZ) used as electrolyte.[1] Temperatures above 800°C are needed to obtain a reasonable ionic conductivity for YSZ. Although the electrolyte can withstand these temperatures, other components like the cathode or metallic interconnect tend to react with the electrolyte, creep or corrode significantly with time.[2] To overcome these problems, which become more and more crucial when long operating times were demanded as for power plants, attempts were made to lower the operating temperature. However, also a lower temperature boundary exists, since the SOFC technology includes the advantage of internal reforming, e.g. fuels like higher carbons can be used directly without the need for additional components like reformer, cracking these fuels first to hydrogen or lower hydrocarbons.[3] This hinders the use of doped ceria, another common electrolyte material, since ceria tends to have partial electronic conductivity for reducing atmospheres above 600°C.[4] An operating temperature of about 700°C is aimed, where a trade-off between materials cost and electrical performance can be made. However, other SOFC materials have to be considered for this aim, since conventional methods like decreasing the electrolyte layer thickness are limited. One of the promising electrolyte materials is scandia-stabilized zirconia (ScSZ).[5] It offers higher ionic conductivity than YSZ at lower temperatures while maintaining other properties like mechanical stability.[6] However, the zirconia-based electrolyte materials show mostly chemical reactions with perovskite materials used as cathode material.[7] Especially for strontium and cobalt doped lanthanum ferrites (LSCF, LaSrCoFe), protective layers have to be introduced to suppress or reduce the formation of insulating secondary phases.[8] A copper and strontium doped lanthanum ferrite (LaSrCuFe) was found to be a promising alternative to LaSrCoFe.[9] Therefore, the combination of the ScSZ with LaSrCuFe was examined to investigate its usability for long-term operated applications.

†Corresponding author : Jürgen Wackerl
E-mail : j.wackerl@fz-juelich.de
Tel : +49-2461-61-6228 Fax : +49-2461-61-3699

2. Experimental Procedure

The electrolyte material ScSZ:Mn with the chemical composition to $(Sc_2O_3)_{0.10}(ZrO_2)_{0.89}(MnO_2)_{0.01}$ was prepared using a spray-pyrolysis method. Pellets of 20 mm diameter and approximately 1 mm thickness were pressed uniaxially with 125 MPa and then sintered at 1400°C for 6 h. The pellets were cut to square shaped samples to 10×10 mm and ground to a thickness of 1 mm. Surface finishing was carried out using grinding paper with 2400 grid. Platinum as anode electrode was sputtered in 2 steps to a total thickness of about 150 nm. A LaSrCuFe perovskite material with the nominal chemical composition to $(La_{0.70}Sr_{0.30})(Cu_{0.20}Fe_{0.80})O_{3-\delta}$

was used as cathode electrode material. It was prepared using the solid state reaction method and calcined at 950°C and subsequently ball-milled. The powder was then partially pre-sintered at 1200°C and thereafter milled and mixed with the remaining calcined material to get a multimodal fractioned powder. To get a paste, this was mixed with a carboxy-methyl-cellulose (CMC) solution acting as binder and pore former. The LaSrCuFe paste was applied on the cell to a thickness of about 200 μm and the complete cell was heat threatened at 900°C for 2 h in air.

The cell was mounted in a furnace using a 4 point - 2 electrode setup. Platinum paste and multiple platinum meshes were used to optimize the electrical contacts and mechanical loading. For the long-term testing, the assembly was heated to 800°C in air and a constant current of 200 mA was maintained. Additionally, the cell voltage was monitored for the complete testing period. The current was interrupted only for impedance measurements, which were carried out to gather additional information. These and other electrical test were carried out using a Solartron 1260 and Solartron 1286 combination (Solartron Analytical, UK) and an Ivium-stat (Ivium Technology, NL) testing device. The processing of the impedance data and modelling was carried out using the DOS-Version of the EquiVCRT program from Boukamp.[10,11]

3. Results

3.1. Electrical tests

The monitored resistance shows an exponential like decrease with time for the first 600 h of testing as shown in Fig. 1. A minimum DC resistance of the cell to 5.7 Ohm (per cm²) was reached after 1300 h. However, the DC resistance of the cell increased asymptotically to a final value of 5.9 Ohm (per cm²) starting after 1500 h of testing. Since the current was kept constant to 200 mA, the voltage over the cell increased therefore. Nevertheless, the voltage across the cell did not exceed a critical value, at which decomposition of any component might occur. This was verified by pretests carried out.

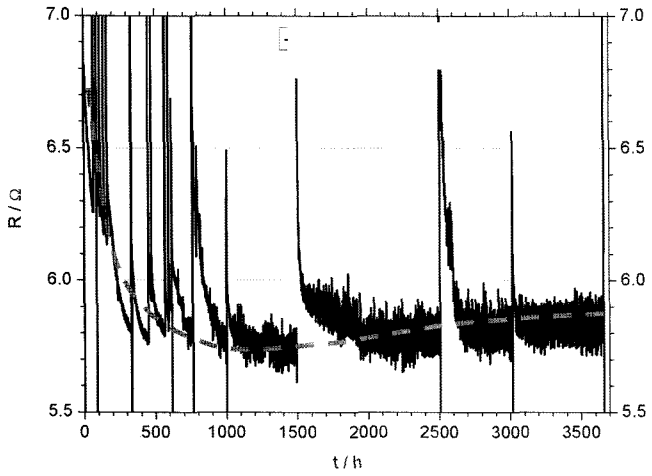

Fig. 1. DC Resistance of a cell operated for more than 3500 h. The dashed line is for optical guideline.

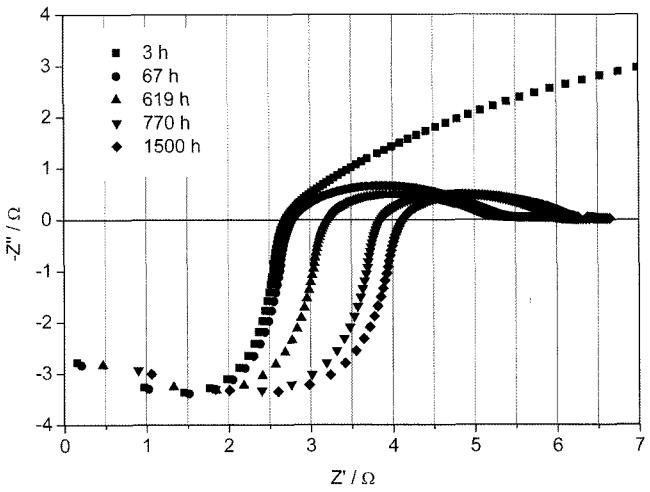

Fig. 2. Selected impedance spectra of a cell obtained for different measurement times.

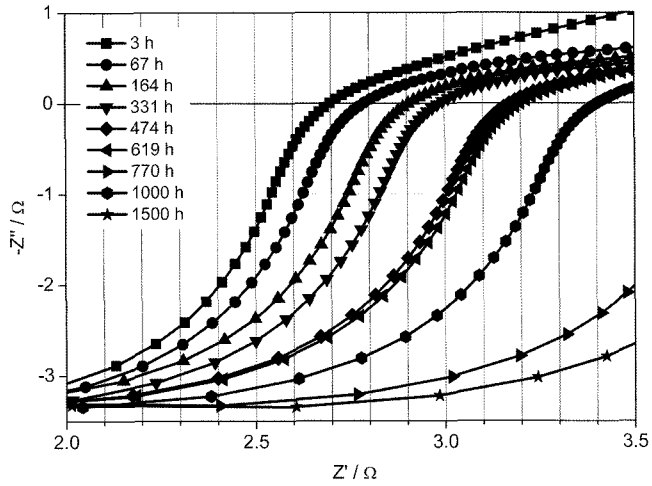

Fig. 3. Magnified impedance area of selected spectra showing the increase of cell resistance with time.

The impedance spectra obtained for several times help to identify the reasons for the DC behaviour. Selected impedance data are shown in Fig. 2. The examined cell shows high impedance especially at low measuring frequencies (LF) for the first measurement after 3 h at 800°C. The subsequent measurements then show apparently a nearly constant low frequency contribution with an increasing high frequency (HF) contribution. This becomes more striking, when the middle and high frequency part of the impedance spectra are compared as shown in Fig. 3. An investigation of the single spectra reveals a problem arising from polarization effects. A selected single spectrum is given in Fig. 4. Especially the LF part, which can be interpreted by anode processes,[12] is affected by slow temporal polarization issues. The longer the cell stays off without applied current, the smaller the effect of temporal shift is. Nevertheless, an

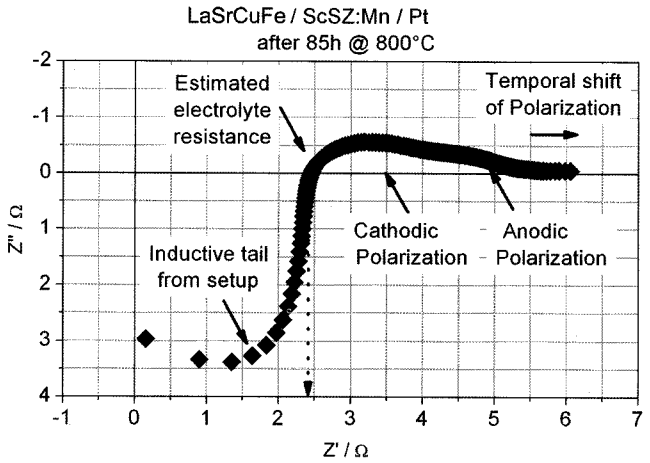

Fig. 4. Contributions to the integral, measured impedance spectra and possible interpretations thereof.

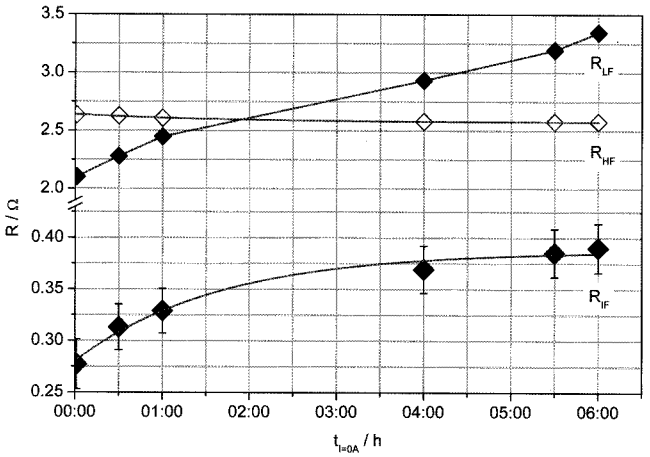

Fig. 5. The temporal change of the resistance modelling parameters after current switching off for a testing time of approximately 1250 h. The connecting lines are optical guidelines.

equivalent electrical circuit in the form

$$L(R_{HF}C_{HF})(R_{IF}C_{IF})(R_{LF}Q) \quad (1)$$

can be used for modelling. L represents the inductance introduced by the setup, R the different resistances, C the corresponding capacitances and Q a constant phase element. The indices HF, IF and LF indicate the frequency range - high, intermediate and low, respectively - where the modelling parameters influence the total impedance spectra most. By applying this formula on the measured impedance data, three main processes could be separated.

To investigate the influence of polarization, the cell was measured using impedance spectroscopy after turning off the current. The obtained calculated resistance contributions are given in Fig. 5. The main temporal effect is observed for the LF contribution, which can be assigned to anode processes.[13] The HF and intermediate frequency (IF) contributions are also affected, but to a much less extent. Additionally, a simple exponential decay and increase could

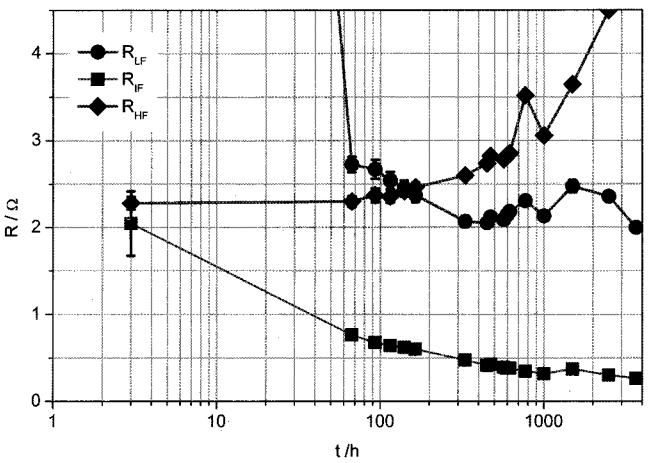

Fig. 6. The development of the fitted high, intermediate and low frequency (HF, IF, LF) resistance contribution of the impedance spectroscopy data for the total measurement period. The connecting lines are optical guidelines.

be applied to the HF and IF data respectively, while the situation is more complex for the LF resistance data. This indicates that the time point of measurement affects severely the results. To obtain most realistic data for the current-on state, impedance measurements were carried out as fast as possible after current switching off.

The development of the calculated HF, IF and LF resistance data for the complete testing period is given in Fig. 6. Different behaviours were found for each contribution. The LF resistance shows a high initial value stabilizing after about 300 h. Since this represents most likely the anode process(es), this indicates a stable anodic conversion performance. The IF resistance shows a decrease over the complete testing period. Since this contribution can normally be assigned to cathode processes,[13] an improvement of cathode performance with time can be assumed. This also means that no severe chemical reactions are apparent at the cathode side, since these would directly affect the cathode electric properties. The HF resistance in contrast shows in the first 200 h a stable value and then increases steadily. Normally, the HF resistance is attributed to the electrolyte resistance. However, it should be considered that in this parameter also all pure ohmic resistances of the cell components are summarized. An explicit assignment to a specific cell component can therefore not be given.

From the two IF model parameters resistance R_{IF} and capacitance C_{IF} the time constant τ is calculated according to:

$$\tau_{IF} = (R_{IF}C_{IF}) \quad (2)$$

According to this parameter, as given in Fig. 7, the decrease in resistance for the cathode is related to a faster getting process, e.g. the conversion or possibly the ionic conduction of the cathode enhances with time.

Since the cell was operated in air for both electrodes, cyclic voltammetry measurements (CV) were carried out. These

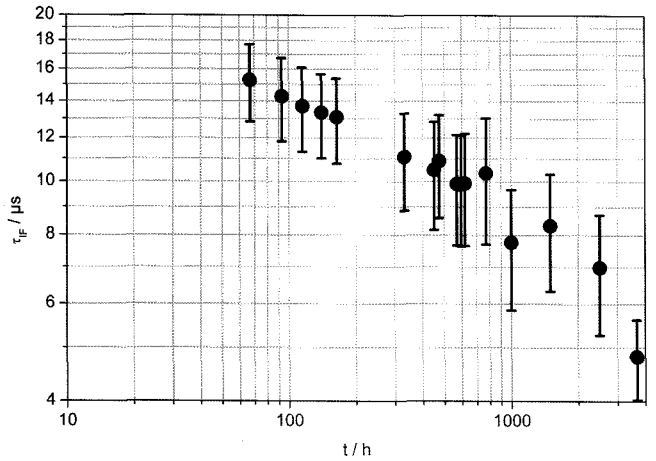

Fig. 7. The calculated time constant τ derived from the IF model parameters.

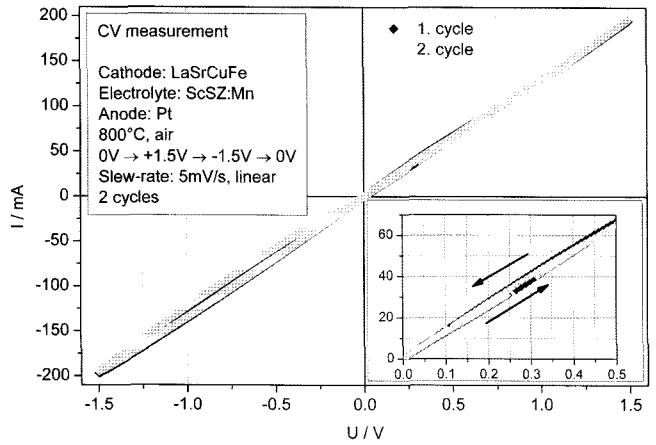

Fig. 8. Current-voltage measurement, subsequent cycles show similar behaviour.

measurements should indicate whether the LaSrCuFe is superior to platinum as cathode material. A typical measurement is given in Fig. 8. When the cell is operated in the forward mode, e.g. the LaSrCuFe acts as cathode, a small hysteresis is found in the voltage range between +0.1 V and +0.5 V which gets less pronounced the more cycles were measured. In the reverse mode, where the Pt acts as cathode, such a hysteresis is also present. However, this span is more expressed than in forward mode. Additionally, the hysteresis is found for the nearly complete measurement range down to −1.5 V. This behaviour is found for a wide temperature as determined at the end of the testing period and given in Fig. 9. Comparing the curves for the different temperatures, the differences between forward and reverse operation of the cell becomes more apparent with decreasing temperature. For a voltage of 1 V par example, the current at 800°C is only 50% higher in forward operation than in reverse. At lower temperatures this gain increases up to more than 100%, even for temperatures down to 550°C. This indicates that the LaSrCuFe as cathode material is superior to platinum.

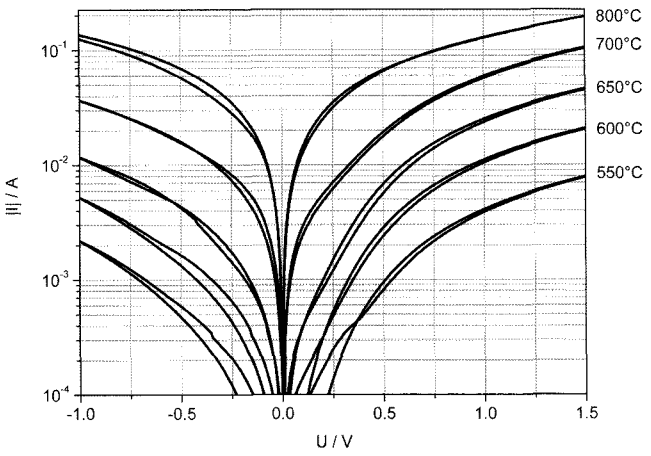

Fig. 9. Current-voltage measurement for different temperatures at the end of the testing period.

3.2. SEM images

Scanning electron microscopy (SEM) images were taken from the samples after testing. A special area of interest of the cathode side is shown in Fig. 10. The only secondary phase found at the interface was copper oxide. Although energy dispersive X-Ray analysis (EDX) was used to identify the different phases, a precise stoichiometry of the copper oxide cannot be given. Since this oxide might have been formed upon cooling of the cell, the oxygen content might have been changed. During the testing, these copper oxide particles might also be metallic copper. However, to check this, in-situ identification must be carried out, which is a demanding task. Nevertheless, these copper precipitations were not found all along the cathode-electrolyte interface. Most of the connections between LaSrCuFe and ScSZ:Mn are of direct nature. No indication for the formation of lanthanum zirconates, as usually expected for lanthanum based perovskites, were found. Using EDX on the electrolyte side of the interface, no significant diffusion of the cathode elements into the electrolyte was found.

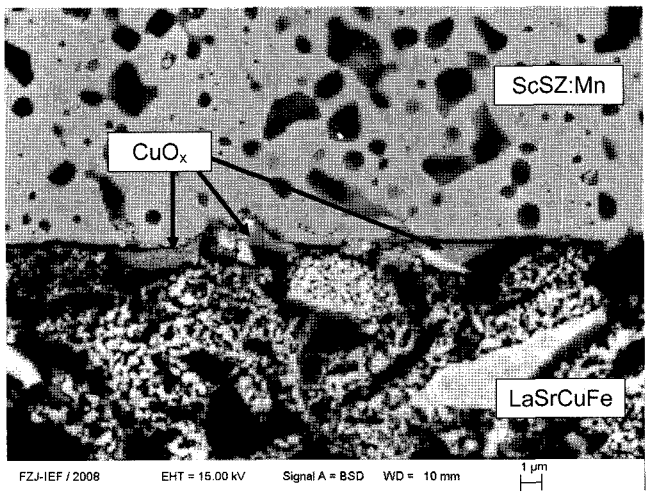

Fig. 10. SEM image of the cathode side after the testing period of 3600 h at 800°C in air.

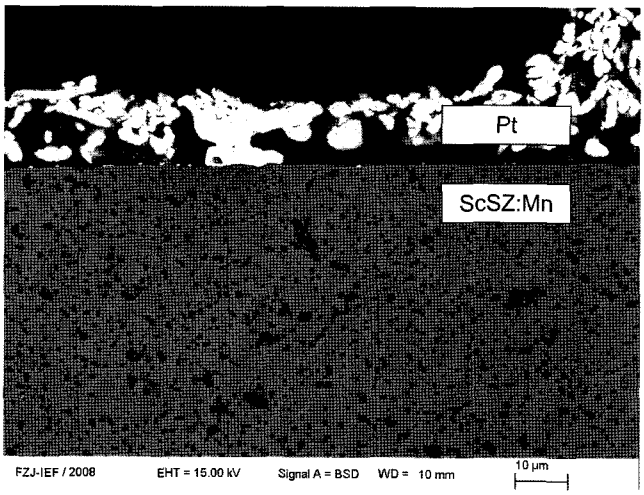

Fig. 11. SEM image of the anode side after the testing period of 3600 h at 800°C in air.

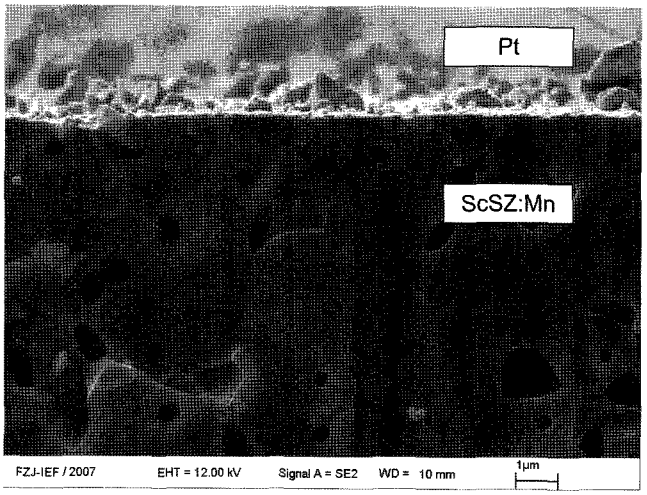

Fig. 12. SEM image of the fracture surface of a single time sputtered platinum anode layer before the testing.

Another interesting point is the morphology of the cathode layer. Although the cell was operated at 800°C for more than 3500 h with additional electrical current, the fine particles of the cathode material were still present. Even very fine cathode particles could be identified within open pores of the electrolyte. Although the shape of the particles indicates some sintering activity - all smaller ones have a spherical geometry -, a coarsening or coagulation to larger bulky structures is not taking place.

The situation is different for the anode-electrolyte interface as shown in Fig. 11. Compared to the initial state as given exemplarily in Fig. 12, the dense sputtered platinum layer vanished. A coarsening of the platinum grains is observed, especially close to the electrolyte surface. The main aspect is the large distance between the contacts between the platinum and the ScSZ:Mn. However, no diffusion of platinum into the electrolyte material was found, even in areas with larger contact areas.

Table 1. Equilibrium Partial Pressure of Various Platinum Species at 800°C Calculated Using FactSage.

Component	O	Pt	PtO	PtO_2
Partial pressure [bar]	$\sim 10^{-9}$	$\sim 2 \cdot 10^{-20}$	$\sim 10^{-17}$	$\sim 10^{-8}$

4. Discussion

When only the data of the DC measurements were considered, a degradation of the cell could be assumed. After an initial phase of approximately 500 h, the cell resistance shows a minimum. With the SEM images showing the initial and final structure of the anode layer, one can explain this by a change of the platinum anode layer. The initial dense and therefore also relative gastight layer becomes partially thinner due to grain growth and relocation. Therefore the oxygen transport through this layer is improved. When holes in the platinum layer were formed as a consequence of the relocation process, optimal conditions were reached: good electrical transverse conductivity to the attached platinum meshes and a sufficient high uncovered surface to provide long triple phase paths (Pt / ScSZ:Mn / gas phase) for the oxygen ion-to-molecule conversion. However, the relocation process does not stop and the uncovered area increases with time, while even electrically isolated platinum isles can be formed.[14,15]

Additionally to this effect, the evaporation of platinum in oxygen rich atmosphere has to be considered.[16] Two oxides of platinum are known: PtO and PtO_2.[17] A rough calculation of the equilibrium partial vapour pressures of these species at the testing conditions from thermo-dynamical data using FactSage is given in Table 1. According to these data, PtO_2 is the more volatile species for this condition and promotes the platinum loss of the anode layer. Additionally, it has to be considered that an electrical current is present, pumping oxygen to the triple phase boundary and therefore increasing locally the oxygen partial pressure respectively its activity. Even higher oxygen partial pressures compared to the one in air have therefore to be regarded. This enhances the reaction between oxygen and platinum towards the formation of more oxides, thus also increasing the vapour pressure thereof. If a dual chamber setup is used with a low oxygen partial pressure on the platinum anode side, this effect would be less pronounced - if not even suppressed - and the evaporation of platinum could most likely be neglected.

Therefore, at least these two processes affect the long-term performance of the anode in air. This can be confirmed using the fitted resistance values from the impedance measurements. The LF resistance R_{LF} as shown in Fig. 6, which is an indicator for the slow anode processes, starts at a high value. Only few sites for the ion-molecule conversion and gas release are available, causing a tailback for oxygen ions transported to the anode and therefore creating a high polarization resistance. Then the R_{LF} decreases rapidly within the first 100 h due to the formation of triple phase

boundaries. The number of conversion sites is therefore increasing, the oxygen ion tailback is reduced and the resulting polarization resistance is governed by other factors. When the uncovered area is increasing, the polarization resistance is only little affected, since the number of oxygen ions per time to be converted is limited by longer oxygen ion transport paths in the electrolyte. This is reflected in the high frequency resistance R_{HF}. After 300 h, this value increases steadily while it was stable before. As already mentioned, this parameter comprises all pure ohmic contributions of the components, but also the ion conductivity of the electrolyte. The latter one was found to be only little affected by aging for similar electrolyte materials.[5] Taking the degree of contact loss at the end of the long-term testing on the anode side additionally in account, the most likely explanations for the increase of R_{HF} are:

- Increased ohmic resistance of the platinum anode mainly due to reduction of the transversal electronic conduction[18] and decreasing number of contact sites.
- Reducing contact area between anode and electrolyte and therefore increase of local current densities due to increasing uncovered areas, causing higher resistive voltage losses.

Both effects are superimposed, leading to a progressive increase of R_{HF} with time. At first sight, the high value of R_{HF} even the initial state of the test is surprising. For that the SEM images can give some information. They show a high porosity of the electrolyte material. This is a fabrication issue, since the electrolyte powder used is optimized for coating techniques. A higher sintering temperature might lead to a more dense structure. Because of the porosity, the electrolyte resistance will be higher than for a fully dense one. This also leads to a higher voltage drop over the 1 mm thick electrolyte layer. The ScSZ:Mn electrolyte material has an electrical conductivity to about 0.1 Scm^{-1},[19,20] therefore a minimum electrolyte resistance of the cell to 1 Ohm can be expected. The actual resistance is higher, since the porosity has to be considered. Thus the electrolyte resistance of the cell tested contributes to about 50% to the calculated high frequency resistance as shown in Fig. 5 and Fig. 6. The other 50% have to be attributed to other ohmic contributions. A main source might be the platinum used, since a 4-probe-2-point setup was used and several platinum layers were used.

The contact loss on the anode side might also explain the results of the cyclic voltammetry measurements. Despite the hysteresis found for the curves, which is most likely due to redox potentials, different currents for a certain cell voltage for the forward and reverse operation are observed. A possible explanation for this effect might be the spill-over effect as proposed by Luerßen et al.[21] In the reverse mode, oxygen ions are transported from the platinum-electrolyte interface away due to the electrical fields. However, the number of available oxygen ions is limited by the length of the triple phase boundary, surface exchange rate and despite some other parameters also the surface diffusion of adsorbed oxygen. In the forward mode, oxygen ions are pushed to the platinum side also driven by the applied electrical field. In contrast to the reverse mode, adsorbed oxygen molecules can now be pushed over the platinum and - to a certain extent - also over the electrolyte surfaces where they finally desorb. The number of oxygen ions per time can therefore be higher for the forward than for the reverse mode of the cell since more area can be used for desorption and thus also the current is increased for a certain potential. With the same effect, the time dependent results of the impedance data as given in Fig. 5 at least for the R_{LF} can be explained. As Jaccoud states in his work,[22] the oxygen spill-over also enhances the catalytic activity and this promotion can last for several hours after current switch-off.

For the resistive contribution in the intermediate frequency range R_{IF}, the situation is different. This parameter is normally related to cathode processes. The SEM examination did not reveal any significant morphology changes between initial and final state of the cell. However, the electrical performance of the cathode interface improved with time, which can be seen from the decreasing resistance and time constant of the cathode process as shown in Fig. 6 and Fig. 7, respectively. Since the cathode layer was sintered on the electrolyte at a rather low temperature to 900°C and the cell was tested at 800°C, sintering effects might have improved the contact between cathode and electrolyte during testing. However, better attached cathode particles and more contact sites would decrease the resistance, but not the time constant, since this is mainly related to the electrochemical processes rather to active area - unless some limiting factors were reached. Indeed, the time constant also decreases with time, e.g. the cathode processes proceed faster. This can for example be obtained by an increased catalytic activity. Since copper oxide precipitations were found along the cathode-electrolyte interface for the SEM images and copper and its oxides are known to show high catalytic activity for oxygen,[23] this seems to be the most reasonable explanation. For the relaxation issues found on short-term as shown in Fig. 5, another property of LaSrCuFe has to be considered. Since this cathode material is of perovskite structure with varying oxygen stoichiometry depending on temperature and oxygen partial pressure, also the electrical conductivity changes.[9] By applying electrical current on the cell, the oxygen content of the gas and solid phase is locally changed. With this change, also the oxygen stoichiometry of the perovskite is altered. Since the resistance increases with promoting relaxation, the oxygen stoichiometry of the perovskite should decrease, e.g. more oxygen vacancies were created to reach an equilibrated state. This again indicates that the cathode material LaSrCuFe was not the main limiting factor for the electrical conductivity, since more oxygen ions were available for the cathode during DC operation than actually used, e.g. the perovskite structure was at least partially saturated. On relaxation, the surplus of oxygen is released off the perovskite and the electrical resistance increases. Another indica-

tion for such a process is the exponential increase of the resistance, which can be related to diffusion effects.

5. Conclusions

For the first time, the combination of a manganese doped scandia-stabilized zirconia (ScSZ:Mn) electrolyte with a strontium and copper doped lanthanum ferrite was examined as possible material combination for a solid oxide fuel cell operated at 750°C or below.

A LaSrCuFe-ScSZ:Mn-Pt cell was successfully operated for more than 3500 h at 800°C in air. The cell was operated with polarization, e.g. a constant current was applied with a nominal current density to 0.2 Acm^{-2}. The DC resistance of the cell was measured using a 4-probe-2-point setup and monitored for the complete testing period. Electrical impedance measurements were carried out from time to time to identify the degradation mechanisms observed for the DC data. At the end of the test, cyclic voltammetry was applied for different temperatures to investigate the cathode versus anode performance.

The agglomeration and evaporation of the anode material Pt were the main reasons for the degradation observed. The degradation was found to be promoted by the loss of platinum covered area. Therefore an increase of the transversal electrical resistance of the anode but also a reduction of active surface for oxygen ion-to-molecule conversion is the consequence. This leads to an increase of ohmic and polarization resistances with time, especially on long-term.

For the cathode, an improvement over the complete testing period of the electrical performance was found. No secondary phases or precipitations despite copper oxides were formed at the cathode-electrolyte interface. Additionally, only little sintering effects are observed for the LaSrCuFe cathode despite the high operation temperature. Therefore the improvement of electrical performance is believed to have its origin in the formation of the copper oxides, enhancing the catalytic activity for oxygen. This assumption is supported by additional cyclic voltammetric measurements carried out, showing higher currents for the LaSrCuFe as cathode than platinum, especially for temperatures below 800°C.

The electrolyte did not show any significant morphological changes after the 3500 h of testing. Additionally, no diffusion of platinum or elements of the cathode into to the electrolyte material were detected. Although no direct conclusion can be drawn from the electrical measurements for the electrolyte material, there are no obvious indications for degradation thereof.

Therefore, the ScSZ:Mn electrolyte / LaSrCuFe cathode combination seems to be interesting for temperatures below 800°C. However, long-term testing has to be carried out using a dual-chamber setup in order to avoid misleading results from unrealistic anode operating conditions, especially if platinum is used as anode material.

Acknowledgment

Thanks go to all people directly and indirectly involved in this work, especially to Dr. E. Wessel for the SEM images, to Prof. K. Hilpert (†) and Dr. T. Markus. The financial support of this work by KIER is greatly acknowledged.

REFERENCES

1. J.W. Fergus, "Electrolytes for Solid Oxide Fuel Cells," *J. Power Sources*, **162** [1] 30-40 (2006).
2. J.W. Fergus, "Materials Challenges for Solid-oxide Fuel Cells," *JOM Journal of the Minerals, Metals and Materials Society*, **59** [12] 56-62 (2007).
3. H. Tu and U. Stimming, "Advances, Aging Mechanisms and Lifetime in Solid-oxide Fuel Cells," *J. Power Sources*, **127** [1-2] 284-93 (2004).
4. S.M. Haile, "Fuel Cell Materials and Components," *Acta Mater.*, **51** 5981-6000 (2003).
5. O. Yamamoto, Y. Arati, Y. Takeda, N. Imanishi, Y. Mizutani, M. Kawai, and Y. Nakamura, "Electrical Conductivity of Stabilized Zirconia with Ytterbia and Scandia," *Solid State Ionics*, **79** 137-42 (1995).
6. M. Hirano, S. Watanabe, E. Kato, Y. Mizutani, M. Kawai, and Y. Nakamura, "High Electrical Conductivity and High Fracture Strength of Sc_2O_3-Doped Zirconia Ceramics with Submicrometer Grains," *J. Am. Ceram. Soc.*, **82** [10] 2861-4 (2004).
7. H. Yokokawa, "Understanding Materials Compatibility," *Annu. Rev. Mater. Res.*, **33** 581-610 (2003).
8. D. Perednis and L.J. Gauckler, "Solid Oxide Fuel Cells with Electrolytes Prepared Via Spray Pyrolysis," *Solid State Ionics*, **166** [3-4] 229-39 (2004).
9. J. Wackerl, Untersuchungen zum Einsatz neuer Werkstoffe für SOFC-Anwendungen (in German), in Dr.-Ing. Thesis, Rheinisch-Westfälische Technische Hochschule Aachen (RWTH), Aachen, 2007.
10. Equivalent Circuit (EquiVCRT) 4.51, B.A. Boukamp, 1989.
11. B.A. Boukamp, "A Nonlinear Least Squares Fit procedure for analysis of immittance data of electrochemical systems," *Solid State Ionics*, **20** [1] 31-44 (1985).
12. S. Primdahl and M. Mogensen, "Mixed Conductor Anodes: Ni as Electrocatalyst for Hydrogen Conversion," *Solid State Ionics*, **152-153** 597-608 (2002).
13. T. Kato, K. Nozaki, A. Negishi, K. Kato, A. Monma, Y. Kaga, S. Nagata, K. Takano, T. Inagaki, H. Yoshida, K. Hosoi, K. Hoshino, T. Akbay, and J. Akikusa, "Impedance Analysis of a Disk-type SOFC using Doped Lanthanum Gallate under Power Generation," *J. Power Sources*, **133** 169-74 (2004).
14. S.L. Firebaugh, K.F. Jensen, and M.A. Schmidt, "Investigation of High-Temperature Degradation of Platinum Thin Films with an *In Situ* Resistance Measurement Apparatus," *J. Microelectromechanical Systems*, **7** [1] 128-35 (1998).
15. J.-S. Lee, H.-D. Park, S.-M. Shin, and J.-W. Park, "Agglomeration Phenomena of High Temperature Coefficient of Resistance Platinum Films Deposited by Electron Beam Evaporation," *J. Mater. Sci. Lett.*, **16** [15] 1257-9 (1997).

16. P.K. Handa and J.C. Matthews, "Modeling of Sintering and Redispersion of Supported Metal Catalysts," *AIChE J.*, **29** [5] 717-25 (1983).
17. J.C. Chaston, "The Oxidation of the Platinum Metals," *Platinum Met. Rev.*, **19** [4] 135-40 (1975).
18. S. Messaadi, C. Pichard, and A.J. Tosser, "Reinterpretation of Thickness-dependent Conductivity of thin Platinum Films," *J. Mater. Sci. Lett.*, **5** [9] 873-5 (1986).
19. D.-H. Peck, R.-H. Song, J.-H. Kim, T.-H. Lim, D.-R. Shin, D.-H. June, and K. Hilpert, "Electrical Conductivity of Scandia Stabilized Zirconia for Membranes in Solid Oxide Fuel Cells," in SOFC-IX, Quebec, Canada, Proceedings - Electrochemical Society (2005).
20. Z. Lei and Q. Zhu, "Phase Transformation and Low Temperature Sintering of Manganese Oxide and Scandia Co-doped Zirconia," *Mater. Lett.*, **61** [6] 1311-4 (2007).
21. B. Luerßen, E. Mutoro, H. Fischer, S. Günther, R. Imbihl, and J. Janek, "In Situ Imaging of Electrochemically Induced Oxygen Spillover on Pt/YSZ Catalysts," *Angew. Chem., Int. Ed.*, **45** [9] 1473-6 (2006).
22. A. Jaccoud, Electrochemical promotion of Pt catalysts for gas phase reactions. (in English), in Ph.D. Thesis, École Polytechnique Fédérale de Lausanne (EPFL), Lausanne, 2007.
23. W.-P. Dow and T.-J. Huang, "Yttria-Stabilized Zirconia Supported Copper Oxide Catalyst II. Effect of Oxygen Vacancy of Support on Catalytic Activity for CO Oxidation," *J. Catal.*, **160** [2] 171-82 (1996).